

Membrane-Bound Plasma Platelet Activating Factor Acetylhydrolase Acts on Substrate in the Aqueous Phase

Jung-Hyun Min,[‡] Mahendra K. Jain,[§] Cheryl Wilder,^{||} Leland Paul,^{||} Rafael Apitz-Castro,[⊥] Daniel C. Aspleaf,[▽] and Michael H. Gelb^{*,‡,▽}

Departments of Biochemistry and Chemistry, University of Washington, Seattle, Washington 98195, Department of Chemistry and Biochemistry, University of Delaware, Newark, Delaware 19716, ICOS Corporation, Bothell, Washington 98021, and Instituto Venezolano de Investigaciones Cientificas, Caracas, Venezuela

Received May 18, 1999; Revised Manuscript Received July 21, 1999

ABSTRACT: Human plasma platelet activating factor acetylhydrolase (pPAF-AH) is a phospholipase A₂ that specifically hydrolyzes the *sn*-2 ester of platelet activating factor (PAF) and of phospholipids with oxidatively truncated *sn*-2 fatty acyl chains. pPAF-AH is bound to lipoproteins in vivo, and it binds essentially irreversibly to anionic and zwitterionic phospholipid vesicles in vitro and hydrolyzes PAF and PAF analogues. Substrate hydrolysis also occurs in the absence of vesicles, with a maximum rate reached at the critical micelle concentration. A novel pre-steady-state kinetic analysis with enzyme tightly bound to vesicles and with a substrate that undergoes slow intervesicle exchange establishes that pPAF-AH accesses its substrate from the aqueous phase and thus is not an interfacial enzyme. Such a mechanism readily explains why this enzyme displays dramatic specificity for phospholipids with short *sn*-2 chains or with medium-length, oxidatively truncated *sn*-2 chains since a common feature of these lipids is their relatively high water solubility. It also explains why the enzymatic rate drops as the length of the *sn*-1 chain is increased. pPAF-AH shows broad specificity toward phospholipids with different polar headgroups. Additional results are that PAF undergoes intervesicle exchange on the subminute time scale and it does not undergo transbilayer movement over tens of minutes.

Platelet activating factor (PAF)¹ is a pair of phospholipids (1-*O*-hexa/octadecyl-2-acetyl-*sn*-glycero-3-phosphocholine) that augments anaphylactic shock, asthma, and allergic reactions and is produced by proinflammatory cells such as endothelial cells, platelets, macrophages, and monocytes (1). In an effort to understand the mechanism of PAF signal termination, efforts turned toward the identification of enzymes that are capable of converting it to inactive 1-*O*-alkyl-*sn*-glycero-3-phosphocholine (phospholipase A₂ class). Three PAF acetylhydrolases that greatly prefer PAF to phospholipids with long *sn*-2 fatty acyl chains have been

cloned (2). The plasma form (pPAF-AH) contains the lipase/esterase GXSG sequence motif with Ser273 as the attacking nucleophile and His351 and Asp296 likely forming the other two elements of a catalytic triad (3).

pPAF-AH is found in the plasma associated with lipoproteins (LDL and HDL) (2). Since this enzyme was purified on the basis of enzymatic activity toward PAF, it is not yet certain whether PAF degradation is its major function. pPAF-AH may also play a role in diminishing oxidative stress because it also prefers phospholipids with oxidatively degraded *sn*-2 acyl chains (2). Interestingly, 4% of the Japanese population has undetectable pPAF-AH activity due to a point mutation (27% heterologous rate), and the pathological consequences of this are being studied (2).

Since naturally occurring long-chain phospholipids have virtually no solubility in water, enzymes such as 14-kDa secreted and 85-kDa cytosolic phospholipases A₂ that act on these substrates must bind to the lipid-water interface. Phospholipid must leave the plane of the bilayer to enter the active-site slot of the bound enzyme (4). An enzyme that must access the substrate from the interface is termed an interfacial enzyme (Figure 1) and is distinguished from an enzyme in the aqueous phase or bound to membranes that accesses its substrate from the aqueous phase (Figure 1, noninterfacial enzyme). Catalysis by a noninterfacial, membrane-bound enzyme can be described by the same kinetic equations that describe the action of an enzyme in the aqueous phase in the absence of an interface with the allowance that the former may be allosterically activated by

* Corresponding author: office phone 206-543-7142; fax 206-685-8665; e-mail gelb@chem.washington.edu

[‡] Department of Biochemistry, University of Washington.

[§] Department of Chemistry and Biochemistry, University of Delaware.

^{||} ICOS Corp.

[⊥] Instituto Venezolano de Investigaciones Cientificas.

[▽] Department of Chemistry, University of Washington.

¹ Abbreviations: C₆-NBD-PC (and -PE, -PS, -PG, and -PA), 1-palmitoyl-2-[6-((7-nitro-2-(1,3-benzoxadiazol-4-yl)amino)caproyl)-*sn*-glycero-3-phosphocholine (and phosphoethanolamine, phosphoserine, phosphoglycerol, and phosphate); C₁₂-NBD-PC, same as C₆-NBD-PC except an *sn*-2 12-aminododecanoyl linker; C₁₀-PAF, 1-decanoyl-2-acetyl-*sn*-glycero-3-phosphocholine (likewise for C₁₂-PAF, C₁₄-PAF and C₂₄-PAF); cmc, critical micelle concentration; DMPC and DMPM, 1,2-dimyristoyl-*sn*-glycero-3-phosphocholine and -methanol; *N*-dansyl-DHPE, *N*-dansyl-1,2-dihexadecyl-*sn*-glycero-3-phosphoethanolamine; pPAF-AH, human plasma platelet activating factor acetylhydrolase; *N*-Rhodamine-PE, *N*-(lissamine rhodamine B sulfonyl)-dioleoylphosphatidylethanolamine; PAF, a mixture of 1-*O*-hexadecyl- and 1-*O*-octadecyl-2-acetyl-*sn*-glycero-3-phosphocholine (C₁₆-PAF and C₁₈-PAF).

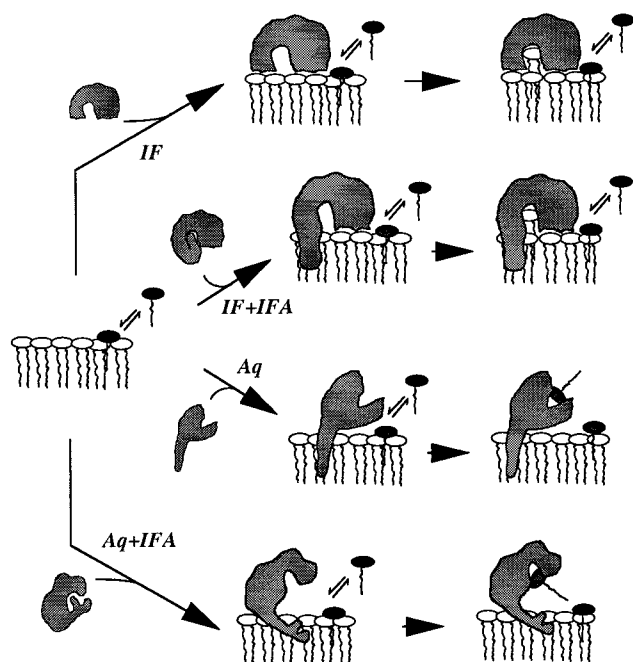


FIGURE 1: Enzymes that act on the membrane–water interface or in the aqueous phase. Water-insoluble phospholipid is shown in white, and a substrate that partitions between the membrane and water phases is shown in black as a single-chain amphiphile. Interfacial mechanism (IF, top line): the water-soluble or water-insoluble enzyme at the interface acts on substrate at the interface (either white or black substrate; only action on white is shown for simplicity). Only substrate in the interface binds to the catalytic site. Interfacial with interfacial activation mechanism (IF + IFA, second line from top): similar to the IF mechanism except that the enzyme undergoes an allosteric transition upon binding to the interface, which increases its catalytic efficiency to act on substrate at the interface. Aqueous mechanism (Aq, third line from top): only substrate in the aqueous phase can bind to the catalytic site of the enzyme at the interface. Aqueous with interfacial activation mechanism (Aq + IFA, bottom line): similar to the Aq mechanism, but enzyme undergoes an allosteric transition upon binding to the interface, which activates it toward the substrate in the aqueous phase.

interaction with the interface, and the membrane phase provides a sink to reduce the concentration of substrate in the aqueous phase. To date, the only unequivocal demonstration that long-chain phospholipid-specific phospholipases A_2 are interfacial enzymes is the observation that they can operate in the scooting mode in which all phospholipid in a single enzyme-containing vesicles is hydrolyzed without transfer of enzyme and phospholipid between vesicles (5, 6).

Since PAF and other substrates for pPAF-AH have finite solubility in water, it is possible that this phospholipase A_2 acts as a membrane-bound, noninterfacial enzyme. Experiments in which one measures the consequences of varying the solution or membrane-phase concentration of substrate on the steady-state rate of the enzymatic reaction cannot distinguish between an interfacial versus a noninterfacial mechanism. This is because the substrate concentrations in the two phases differ only by a constant, the partition equilibrium constant for the transfer of substrate between the aqueous and membrane phases. Thus the velocity equation expressed in terms of concentration of substrate in the aqueous phase has the same form as the equation expressed in terms of the membrane-phase substrate concentration.

In the present study, a number of properties of pPAF-AH are revealed, including its behavior under pre-steady-state conditions, which leads to the conclusion that this enzyme accesses its substrate only from the aqueous phase. This kinetic mechanism readily explains the substrate preferences of pPAF-AH. Kinetic studies were carried out with pPAF-AH in solution or bound to zwitterionic and anionic phospholipid vesicles. Zwitterionic phospholipid vesicles seem like a logical starting point for the detailed mechanistic analysis of pPAF-AH in a well-defined system since the lipid portion of the surface of LDL and HDL, to which the enzyme is bound *in vivo*, is composed of a monolayer of lecithin and sphingomyelin with a minor amount of other phospholipids and free cholesterol (7, 8). Although mutagenesis studies suggest that the C-terminus of LDL-bound apolipoprotein B100 interacts with pPAF-AH and that this may be the basis for association of pPAF-AH with LDL (9), there is no evidence that this protein–protein interaction modulates the kinetics of pPAF-AH catalysis.

MATERIALS AND METHODS

Materials. All phospholipids are from Avanti except DMPM and 1,2-ditetradecyl-*sn*-glycero-3-phosphomethanol, which are from Alexis, and C_{16} -PAF and C_{18} -PAF, which are from BioMol. *p*-Nitrophenyl acetate and butyrate are from Sigma. *N*-Dansyl-DHPE was prepared as described (6). C_{10} -, C_{12} - and C_{24} -PAF were prepared by acetylation of the corresponding lysophospholipids with acetic anhydride in CH_2Cl_2 containing 4-(*N,N*-dimethylamino)pyridine (10) and were purified by flash chromatography over silica gel with a $CHCl_3$ /methanol/water gradient. Bee venom and porcine pancreatic phospholipases A_2 are from Boehringer.

Recombinant pPAF-AH was purified as described (3). For some experiments, a detergent-free preparation was used. This was prepared by applying 4 mg of enzyme to a HP HiTrap SP column (1 mL, Pharmacia) equilibrated with 20 mM MES and 10 mM CHAPS, pH 6.5 at 4 °C. The column was washed with 10 mL of equilibration buffer at 1 mL/min, and enzyme was eluted with 20 mM Tris, 150 mM NaCl, and 10 mM CHAPS, pH 7.5. Finally, enzyme was dialyzed overnight at 4 °C with 10 mM Tris, pH 8.0, and used within 1 day while stored on ice.

CMC Determinations. CMCs of lipids were determined by dynamic light scattering or by the surface tension method (both done in 1 mM NaCl at 21 °C). Light scattering was carried out with a Spectra-Physics helium–neon gas laser (model 125A) with a scattering angle of 90° and a sample volume of 10 mL. Surface tension measurements were made with a Cahn dynamic contact angle analyzer (Model DCA-312, Cahn Instruments Inc.) with a sample volume of 5 mL.

Enzyme Kinetic Studies. Unless stated otherwise, pH-stat reaction mixtures (11) contained 5 mL of 1 mM NaCl, pH 8.0, at 21 °C and other additives as indicated in the figure legends. Fluorescence experiments with NBD phospholipids were carried out in 2 mL of 10 mM Tris-HCl, pH 8.0, at 21 °C with magnetic stirring. Sonicated small unilamellar vesicles for kinetic and binding studies were prepared as described (11). Vesicles were either used on the same day or frozen and resonicated on the day of use. Large unilamellar vesicles were prepared as described (6) and used within 1 day. Hydrolysis of *p*-nitrophenyl esters was monitored at 400 nm in 10 mM Tris-HCl, pH 8.0, at 20 °C.

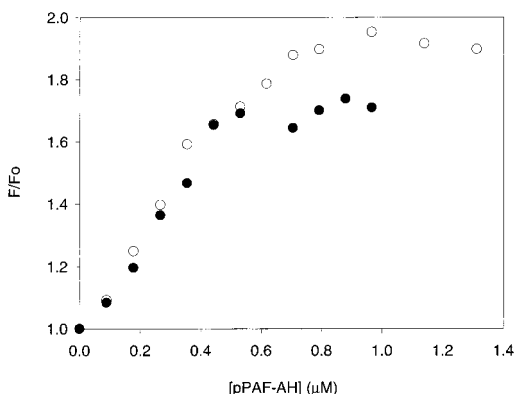


FIGURE 2: Binding of pPAF-AH to vesicles. Mixtures contained DMPM (○) or DMPC (●) sonicated vesicles (30 μ M lipid, both with 3 mol % *N*-dansyl-DHPE) and energy transfer was monitored following the addition of the indicated amount of enzyme (F is the emission with all components and F_0 is the emission with vesicles only).

Intervescle Exchange of Phospholipids. A stock solution of 10 mM DMPM containing 0.25 mM C_6 -NBD-PC or C_{12} -NBD-PC and 0.25 mM *N*-rhodamine-PE was diluted into 2 mL of 10 mM Tris-HCl, pH 8.0, to give a final DMPM concentration of 50 μ M. Acceptor DMPM vesicles were added from a 10 mM stock to 50 μ M. The solution was stirred at 21 $^{\circ}$ C, excitation was at 480 nm, and emission was monitored at 540 nm (12).

Vesicle Binding Studies. Binding reactions contained 1 mL of 10 mM Tris-HCl, pH 8.0, at 28 $^{\circ}$ C, various concentrations of sonicated phospholipid vesicles containing 3 mol % *N*-dansyl-DHPE, and other components as indicated in the figure legend. Excitation was at 292 nm, and emission was from 300 to 600 nm. A long-pass, 335 nm cutoff filter was placed between sample and emission monochromator to prevent scattered light at 292 nm from entering the monochromator.

RESULTS

Binding of pPAF-AH to Vesicles. pPAF-AH is mostly bound to LDL and HDL in plasma (2), which suggests that pPAF-AH may bind to phospholipid vesicles. Such a proposal seems reasonable given that, under physiological conditions, most of the PAF is presumably partitioned into membrane interfaces. To explore the interfacial binding properties of pPAF-AH we used a spectrofluorometer to measure resonance energy transfer from one or more enzymic tryptophans to the probe *N*-dansyl-DHPE present as a minor component in vesicles. As shown in Figure 2, addition of increasing amounts of pPAF-AH to a fixed amount of anionic DMPM/*N*-dansyl-DHPE or zwitterionic DMPC/*N*-dansyl-DHPE vesicles leads to an increase in energy transfer until a maximal amount of enzyme is loaded onto vesicles. With both anionic and zwitterionic vesicles, binding saturation occurs with ~ 30 outer-layer phospholipids per enzyme [assuming 60% of total lipid in the outer layer (13)]. This value is similar to lipid/enzyme ratios of 20–40 measured for 14-kDa secreted phospholipases A_2 by the same method (14, 15). No increase in emission at 508 nm was seen when enzyme was added to vesicles that did not contain *N*-dansyl-DHPE. Similar binding behavior was observed with a detergent-free stock solution of enzyme.

The reversibility of interfacial binding was examined by adding pPAF-AH to *N*-dansyl-DHPE-loaded DMPM or DMPC vesicles (30 μ M lipid) under noncrowded conditions (~ 80 lipids/enzyme) in the presence or absence of 5 mol % C_{18} -PAF and monitoring the change in dansyl emission after the addition of 30 μ M vesicles without fluorophore. No decrease in energy transfer was seen up to 20 min (not shown), indicating that binding of enzyme to both anionic and zwitterionic vesicles is tight (dissociation rate constant of $< 3 \times 10^{-3} \text{ min}^{-1}$). Control experiments showed that addition of enzyme last to a mixture of equal numbers of vesicles with and without fluorophore gave $\sim 50\%$ of the emission measured in experiments in which all vesicles contained fluorophore (not shown). Additionally, no increase in energy transfer was observed over 20 min when DMPM or 1,2-ditetradecyl-*sn*-glycero-3-phosphomethanol vesicles containing 3 mol % *N*-dansyl-DHPE were added to enzyme-containing vesicles without fluorescent lipid. Addition of 0.5 M NaCl did not cause enzyme to desorb from DMPM vesicles; thus, binding of pPAF-AH to anionic vesicles is not predominantly electrostatic in nature. Tight binding of pPAF-AH to vesicles of the diether phospholipid analogue 1,2-ditetradecyl-*sn*-glycero-3-phosphomethanol was also shown by energy transfer experiments (half-time for desorption of enzyme from vesicles > 60 min), showing that enzyme binds tightly to vesicles in the absence of any possible lipolysis. Similar tight binding of enzyme to 1-palmitoyl-2-oleoyl-*sn*-glycero-3-phosphoserine was also observed.

Hydrolysis of PAF and PAF Analogues by pPAF-AH in the Absence of Vesicles. The initial rate of hydrolysis of C_{10} -, C_{12} -, and C_{14} -PAF as a function of the substrate concentration in the absence of vesicles was measured. The cmc of C_{14} -PAF was measured by light scattering and by surface tension, and a value of 14–46 μ M was obtained (Table 1). The published value for C_{14} -PAF is 11 μ M (16). Figure 3 shows that the initial rate of hydrolysis of C_{14} -PAF increases linearly, and then the rate levels off abruptly. The leveling off point occurs at 20 μ M, close to the cmc of C_{14} -PAF. There is no evidence for substrate saturation of the active site of pPAF-AH in the presence of subcritical micellar concentrations of substrates (i.e., $K_M > \text{cmc}$), and thus no attempt was made to obtain K_M and V_{max} by curve fitting to the Michaelis–Menten equation. It may also be noted that it is possible that the enzyme and substrate form a microaggregate in the presence of subcritical micellar concentrations of substrate (17), but this was not investigated. The data in Figure 3 are consistent with an aqueous mechanism for pPAF-AH. If enzyme operates only on substrate in the aqueous phase, the horizontal part of the curve in Figure 3 is due to the fact that the concentration of aqueous-phase substrate does not increase beyond the cmc as more and more lipid is added, and thus the rate does not change. The possibility of an interfacial mechanism for pPAF-AH cannot be conclusively abandoned on the basis of the data in Figure 3. One could argue that more and more enzyme is drawn into protein–lipid microaggregates as the concentration of C_{14} -PAF is increased until all of the enzyme is bound to lipid micelles (linear portion of the curves). At that point, addition of more micelles will not increase the rate further since it will not change the surface concentration of substrate that micellar-bound enzyme encounters (mole fraction 1).

Table 1: Kinetic Parameters for PPAF-AH Acting on PAF and PAF Analogues

substrate (cmc)	no vesicles present		DMPM present		DMPC present	
	V_{\max} (s^{-1})	K_M (μM)	$^aV_{\max}$ (s^{-1})	[S] at 50% $^aV_{\max}$ (μM)	$^aV_{\max}$ (s^{-1})	[S] at 50% $^aV_{\max}$ (μM)
PAF	<i>a</i>	<i>a</i>	16 (15) ^b	44 (24)	15 (14)	11 (4)
C ₁₈ -PAF (0.17 μM) ^c	<i>a</i>	<i>a</i>	2.9 \pm 0.3	26 \pm 7	nd ^d	nd
C ₁₆ -PAF (1.1) ^c	<i>a</i>	<i>a</i>	27 \pm 3	110 \pm 27	nd	nd
C ₁₄ -PAF (14–46, 11) ^c	<i>a</i>	<i>a</i>	61	55 (53, 38)	48 (44)	21 (13)
C ₁₂ -PAF (110) ^c	42 ^e	25 ^e	(48 \pm 2)	(20 \pm 3)	(38 \pm 1)	(14 \pm 1)
C ₁₀ -PAF (> 1000)	39 ^e	73 ^e	36 \pm 1	89 \pm 7	(37 \pm 3)	(51 \pm 14)
1-palmitoyl-2-acetyl-PC	<i>a</i>	<i>a</i>	22 \pm 1	43 \pm 6	nd	nd
1-palmitoyl-2-propanoyl-PC	<i>a</i>	<i>a</i>	13 \pm 2	43 \pm 11	nd	nd
1-palmitoyl-2-nonanoyl-PC	<i>a</i>	<i>a</i>	0.1 \pm 0.02	31 \pm 11	nd	nd
C ₂₄ -PAF	<i>a</i>	<i>a</i>	\sim 0.1	nd	nd	nd
C ₆ -NBD-PC	7 \pm 1	9 \pm 2	3.4 \pm 0.4	35 \pm 12	3.7 \pm 0.5	8 \pm 4
C ₆ -NBD-PE	nd	nd	3 \pm 1	343 \pm 105	2.5 38 \pm 0.3	60 \pm 18
C ₆ -NBD-PS	nd	nd	14 \pm 1	36 \pm 4	7 \pm 2	80 \pm 44
C ₆ -NBD-PG	nd	nd	12 \pm 1	73 \pm 14	11 \pm 2	154 \pm 51
C ₆ -NBD-PA	nd	nd	26 \pm 1	26 \pm 2	23 \pm 5	167 \pm 57

^a No data are given for long-chain substrates for the reasons given in the text. ^b Numbers in parentheses were measured after addition of substrate to preformed vesicles. For all other measurements, vesicle and substrate lipids were cosonicated. ^c Reference 16. ^d Not determined. ^e From the fit of the data in Figure 3 to the Michaelis–Menten equation.

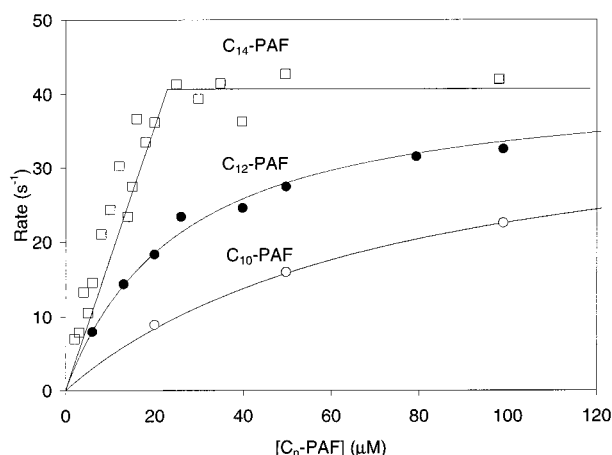


FIGURE 3: Initial velocity (pH-stat) for the hydrolysis of C₁₀-, C₁₂-, and C₁₄-PAF by pPAF-AH as a function of substrate concentration in the absence of phospholipid vesicles.

Figure 3 also shows rate versus substrate concentration data for C₁₀- and C₁₂-PAF. The published cmc for C₁₂-PAF is 110 μM (16). An attempt to measure the cmc of C₁₀-PAF showed that the dye fluorescence increased linearly as the concentration of lipid was increased from 0 to 1 mM with no abrupt jump in fluorescence. This suggests that C₁₀-PAF does not form well-defined micelles below 1 mM. Figure 3 shows that the initial velocity for the hydrolysis of C₁₀-PAF and C₁₂-PAF by pPAF-AH increases in a hyperbolic manner with substrate concentrations below their cmcs. V_{\max} and K_M values are given in Table 1. In studies with C_{10–14}-PAF, all of the substrate becomes hydrolyzed at the end of the reaction.

Hydrolysis of PAF and PAF Analogues by pPAF-AH in the Presence of Vesicles. The hydrolysis of PAF and PAF analogues by pPAF-AH was also studied in the presence of 385 μM DMPM or DMPC vesicles. Consistent with earlier kinetic studies (2), pPAF-AH shows progressively lower activity with phosphatidylcholine substrates containing increasingly longer *sn*-2 fatty acyl chains. Increasing amounts of substrates were added to DMPM vesicles, and the initial velocities were obtained by use of the pH-stat. Hyperbolic velocity versus amount of substrate plots were obtained in all cases. The apparent maximal velocities ($^aV_{\max}$) and the

concentrations of substrates required to obtain 50% of $^aV_{\max}$ are listed in Table 1. It can be seen that $^aV_{\max}$ decreases with increasing length of the *sn*-2 chain of the substrate. As described in the Discussion section, $^aV_{\max}$ and the concentrations of substrates required to obtain 50% of $^aV_{\max}$ do not have their usual meaning in terms of the Michaelis–Menten equation.

On the basis of cmc measurements (see above), most of the C₁₀-PAF should be in the aqueous phase in the presence of 385 μM phospholipid vesicles. The fact that the V_{\max} values for the hydrolysis of C₁₀-PAF in the presence and absence of vesicles are similar (Table 1) shows that pPAF-AH bound to vesicles has similar catalytic power as the enzyme in solution. For the longer chain substrates, enzymatic rates in the presence of vesicles are lower than in their absence. One possible explanation for this is that pPAF-AH bound to the vesicle interface acts on substrate in the aqueous phase (Aq or Aq + IFA mechanisms, Figure 1) since the concentration of substrate in the aqueous phase will be lower in the presence of vesicles due to partitioning. However, such an argument does not establish an Aq-type mechanism; the lower rates could be due to a combination of an IF-type mechanism and surface dilution of substrates by vesicle phospholipids and/or inhibition of pPAF-AH by vesicle phospholipids.

PAF and additional PAF analogues were studied in the presence of DMPM and DMPC vesicles. Increasing amounts of C_{12–18}-PAFs were added to vesicles, and the initial velocities were obtained by use of the pH-stat. Hyperbolic velocity versus amount of substrate plots were obtained in all cases. Values of $^aV_{\max}$ and the concentrations of substrates required to obtain 50% of $^aV_{\max}$ are listed in Table 1. Surprisingly, it was found that increasing the length of the *sn*-1 chain lowers the observed hydrolysis rate of pPAF-AH-catalyzed lipolysis. As summarized in Table 2, C₂₄-PAF is a very poor substrate for pPAF-AH. In these studies the diether analogue of DMPM, 1,2-ditetradecyl-*sn*-glycero-3-phosphomethanol, was used as the vesicle matrix to reduce background consumption of titrant in the pH-stat due to very slow hydrolysis of DMPM by pPAF-AH (see below). The turnover number of pPAF-AH-catalyzed hydrolysis of C₂₄-

Table 2: Relative Rates of Hydrolysis of PAF and PAF Analogues by pPAF-AH and Secreted Phospholipases A₂^a

enzyme	substrate	velocity relative to C ₁₆ -PAF ^b
pPAF-AH	C ₁₆ -PAF	1.0
	C ₁₈ -PAF	0.083
	C ₂₄ -PAF	0.009
bee venom phospholipase A ₂	C ₁₆ -PAF	1.0
	C ₁₈ -PAF	0.34
	C ₂₄ -PAF	0.79
porcine pancreatic phospholipase A ₂	C ₁₆ -PAF	1.0
	C ₁₈ -PAF	1.1

^a All substrates are present at mole fraction 0.1 in 1,2-ditetradecyl-*sn*-glycero-3-phosphomethanol vesicles. ^b Errors are $\leq 25\%$.

PAF, when present at mole fraction 0.1 in vesicles, is 70-fold and 12-fold lower than the turnover numbers for C₁₆-PAF and C₁₈-PAF hydrolysis, respectively. In contrast, bee venom phospholipase A₂ hydrolyzes C₁₆-, C₁₈-, and C₂₄-PAF with similar rates (maximum variation of 2-fold), and porcine pancreatic phospholipase A₂ hydrolyzes C₁₆- and C₁₈-PAF at the same rate (C₂₄-PAF not tested) (Table 2). These results are consistent with the fact that secreted phospholipases A₂ access substrate in the interface and that the surface concentration of these substrates in the presence of the concentration of vesicles used are approximately invariant to the length of their *sn*-1 acyl chains. The very different behavior of pPAF-AH suggests that this enzyme accesses its substrate from the aqueous phase.

As summarized in Table 1, the concentrations of substrates required to achieve 50% of v_{\max} when PAF or PAF analogue was added last to preformed DMPM or DMPC vesicles are $\sim 50\%$ of the concentrations when substrate and DMPM or DMPC are cosonicated; however, values of v_{\max} do not change. This shows that vesicle-bound pPAF-AH is not accessible to PAF or PAF analogue on the inner layer of vesicles, i.e., that the rate of transbilayer substrate movement is slow on the tens of minutes time scale. The concentrations of substrates required to achieve 50% of v_{\max} but not v_{\max} measured in the presence of DMPC vesicles are smaller than those measured in the presence of DMPM vesicles (Table 1). One explanation for these results is that pPAF-AH operates by an Aq-type mechanism and that PAF and PAF analogues partition into DMPM vesicles more than into DMPC vesicles, leading to a lower aqueous-phase substrate concentration with DMPM.

To determine if PAF analogues partition differentially into DMPM and DMPC vesicles, we used the fluorescent PAF analogue C₆-NBD-PC to measure the distribution of lipid between DMPM and DMPC vesicles (12). These experiments are carried out by measuring NBD fluorescence from vesicles containing C₆-NBD-PC and the nonexchangeable phospholipid *N*-rhodamine-PE as a function of the concentration of acceptor vesicles without fluorophores. Transfer of C₆-NBD-PC to vesicles without *N*-rhodamine-PE relieves quenching of NBD fluorescence by rhodamine. By comparing results obtained with DMPM/*N*-rhodamine-PE/C₆-NBD challenged with DMPC (or DMPC/*N*-rhodamine-PE/C₆-NBD challenged with DMPM), it was concluded that C₆-NBD-PC prefers to partition into DMPM over DMPC vesicles by 2–3-fold (not shown). This differential partitioning could explain

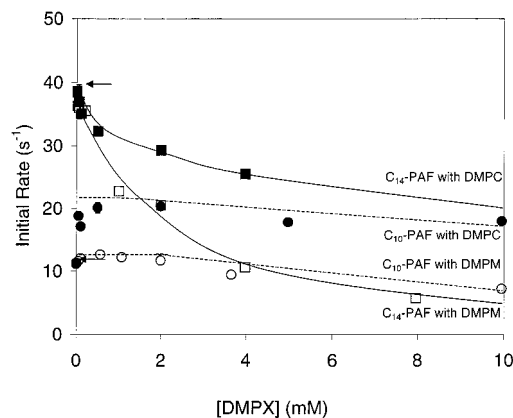


FIGURE 4: Initial velocity (pH-stat) for the hydrolysis of 50 μM C₁₀-PAF (●, ○) or C₁₄-PAF (■, □) versus the concentration of DMPM (open symbols) or DMPC (solid symbols) vesicles. Arrows indicate the rate measured in the absence of vesicles.

the enzymatic velocity trends noted above. Nichols and Pagano (12) have shown that C₆-NBD-PC partitions more favorably into phosphatidylserine and phosphatidic acid vesicles than into zwitterionic phosphatidylcholine vesicles.

It was found that C₆-NBD-PC is hydrolyzed by pPAF-AH with a turnover number comparable to that for C₁₈-PAF (Table 1). This permitted an analysis of the substrate specificity of pPAF-AH with respect to the phospholipid headgroup by using C₆-NBD-PE, -PS, -PG, and -PA (head-group variants of PAF are not readily available). In the presence of DMPM and DMPC vesicles, values of v_{\max} differ only by up to a factor of 10, and the rank order is PC \approx PE < PS \approx PG < PA. For each substrate, v_{\max} values in the presence of DMPM and DMPC are similar, again showing that pPAF-AH bound to both anionic and zwitterionic vesicles displays similar catalytic efficiency. Note that the concentration of C₆-NBD-PE required to achieve half of v_{\max} in the presence of DMPM vesicles is anomalously high, and the value drops 6-fold in the presence of DMPC vesicles (Table 1). C₆-NBD-PA, -PG, and -PS show the opposite but less dramatic behavior: 6.4-, 2.1-, and 1.9-fold higher concentrations needed with DMPC than with DMPM vesicles. DMPM versus DMPC differential partitioning studies, carried out as described above, show that C₆-NBD-PE prefers DMPM over DMPC by 4-fold, whereas C₆-NBD-PA, -PG, and -PS prefer DMPC over DMPM by 2.7-, 2.2-, and 1.7-fold, respectively. This trend seems consistent with the electrostatic effect and accounts for the differences in concentrations of substrates needed to achieve half of maximal pPAF-AH enzymatic velocity (Table 1) if the enzyme is sensitive to the aqueous phase concentration of substrate.

Figure 4 shows the initial velocity for the hydrolysis of a fixed amount of C₁₀- and C₁₄-PAF as a function of the amount of DMPM and DMPC present. The lowest concentration of vesicle lipid used, 50 μM , is sufficient to allow all pPAF-AH to bind under noncrowded conditions. Most of the C₁₀-PAF is in the aqueous phase in the presence of 50 μM vesicle lipid. On the basis of the following arguments, the experiments in Figure 4 do not allow a distinction between the IF, IF + IFA, Aq, and Aq + IFA models. As the concentration of vesicles is increased, the moles of C₁₀-PAF in the interface will increase by the same factor, and thus the interfacial concentration of substrate will not change

much (nor will the aqueous concentration if most of the substrate is in the aqueous phase). For all three models, the enzymatic rate will remain constant until much of the substrate is partitioned into vesicles. Then, increasing the amount of vesicles further will lead to lower vesicle and aqueous-phase concentrations of substrate and the enzymatic rate will decrease. This behavior is observed (Figure 4), and it appears that most of the C_{10} -PAF is present in vesicles when the DMPC concentration is >1 – 2 mM. Qualitatively similar results were obtained with DMPM vesicles except that lower rates were observed (for reasons given above).

Most of the C_{14} -PAF appears to be partitioned into $50\text{ }\mu\text{M}$ DMPC vesicles because only the decreasing limb of the curve is seen (Figure 4). This is the expected behavior for C_{14} -PAF, which has a cmc of 5 – $8\text{ }\mu\text{M}$. Note that the decrease in rate occurs at lower vesicle concentration than with C_{10} -PAF (Figure 4), as expected. Again, the rates in the presence of DMPM are lower than those measured with DMPC for the possible reason stated above. The results in Figure 4 underscore the fact that steady-state kinetic experiments cannot distinguish between interfacial and aqueous mechanisms (see introduction).

We found that the active esters *p*-nitrophenyl acetate and butyrate are substrates for pPAF-AH. Enzyme hydrolyzes $250\text{ }\mu\text{M}$ *p*-nitrophenyl acetate with a rate of $4.1 \pm 0.5\text{ s}^{-1}$, and the rate increases about 70% to $6.9 \pm 0.1\text{ s}^{-1}$ after the addition of $100\text{ }\mu\text{M}$ sonicated DMPM vesicles. With *p*-nitrophenyl butyrate ($250\text{ }\mu\text{M}$), the rate is $10 \pm 1\text{ s}^{-1}$ and $19 \pm 1\text{ s}^{-1}$ without and with $100\text{ }\mu\text{M}$ DMPM vesicles (sonicated or extruded), respectively.

Pre-Steady-State Kinetic Studies with NBD-Phospholipids. The key to determining whether interfacial or aqueous mechanisms apply to pPAF-AH is to measure the reaction under pre-steady-state conditions in which substrate and enzyme do not exchange rapidly between vesicles. Kinetic studies were carried out with the fluorescent phosphatidylcholine analogues C_6 -NBD-PC and C_{12} -NBD-PC. The rate of intervesicle exchange of these substrates can be accurately monitored by fluorescence (12). The half-times for intervesicle exchange of C_6 -NBD-PC and C_{12} -NBD-PC are 0.6 and 60 min, respectively, which agree reasonably well with the published numbers for the same compounds of 0.78 and 150 min (12).

A series of experiments were carried out in which the order of addition of pPAF-AH to DMPM and DMPM/ C_{12} -NBD-PC vesicles was varied, and enzymatic reaction velocities were measured in the pH-stat. A 5 mL reaction mixture at pH 8.0 and $21\text{ }^{\circ}\text{C}$ containing $370\text{ }\mu\text{M}$ DMPM vesicles was placed in the pH-stat cup, and the baseline was recorded for 15 min. Enzyme ($0.082\text{ }\mu\text{M}$) was added, and a slight increase in rate of titrant consumption above the minus-enzyme background rate (presumably due to enzymatic hydrolysis of DMPM) was measured for 24 min (Figure 5, curve a). Under these conditions all of the enzyme is bound to vesicles under noncrowded conditions. Then, a small volume ($200\text{ }\mu\text{L}$) of vesicle stock solution was added to deliver DMPM vesicles containing 5 mol % C_{12} -NBD-PC at a final concentration of $370\text{ }\mu\text{M}$ DMPM, and the rate of titrant consumption was recorded for 25 min. No increase in the rate of titrant consumption was observed (Figure 5, curve a). The experiment was repeated but enzyme was first added to DMPM/ C_{12} -NBD-PC vesicles. Prior to addition of en-

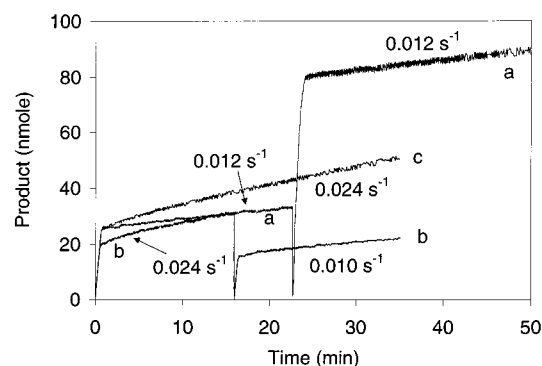


FIGURE 5: Reaction progress curves (pH-stat) for the hydrolysis of NBD phospholipids in the presence of DMPM vesicles: curve a, pPAF-AH was added to $385\text{ }\mu\text{M}$ DMPM vesicles at time zero and $385\text{ }\mu\text{M}$ DMPM/5 mol % C_{12} -NBD-PC was added after 22 min; curve b, pPAF-AH was added to DMPM/ C_{12} -NBD-PC vesicles at time zero, and DMPM vesicles were added at 16 min; curve c, pPAF-AH was added to DMPM/ C_{12} -NBD-PC vesicles at time zero. The sharp, near-vertical jumps are due to the slight acidity ($\text{pH} < 8$) of the components added to the reaction mixture.

zyme, vesicles were incubated in the pH-stat cup for 20 min. After 15 min, a small volume ($200\text{ }\mu\text{L}$) of vesicle stock solution was added to deliver DMPM without C_{12} -NBD-PC at a final concentration of $370\text{ }\mu\text{M}$, and as shown in Figure 5 (curve b), the rate of titrant consumption decreases immediately to that measured for the action of enzyme measured on DMPM vesicles alone (curve a). This decrease in rate cannot be due to substrate dilution by buffer addition since the addition of the second vesicle solution increases the reaction volume only by 4%. As a control, it was shown that the reaction continues at the same rate if the second addition of DMPM vesicles is not made (Figure 5, curve c). Given the low concentration of substrate in the aqueous phase, this reaction progress requires in part replenishment of aqueous-phase substrate by desorption of C_{12} -NBD-PC from vesicles. The measured desorption rate for this phospholipid (see above) is fast enough to account for this reaction progress. The low initial velocity seen in Figure 5, curve a, is the result of the low aqueous concentration of C_{12} -NBD-PC just after the stock solution of DMPM/ C_{12} -NBD-PC is diluted into the reaction mixture. The experiments in Figure 5 were reproducibly obtained in five independent trials. In these experiments, the slow hydrolysis of DMPM by pPAF-AH is of no consequence since only a small fraction of vesicle DMPM is hydrolyzed during the course of the kinetic measurements, and thus the vesicle integrity is maintained.

These results rule out the IF and IF + IFA mechanisms. If vesicle-bound pPAF-AH is acting on C_{12} -NBD-PC in the interface, the initial reaction rate should not decrease upon addition of vesicles without substrate because it takes tens of minutes for the surface concentration of C_{12} -NBD-PC to drop in enzyme-containing vesicles. On the other hand, if vesicle-bound enzyme acts on substrate in the aqueous phase, the rate should drop virtually immediately after the addition of DMPM vesicles since the solution concentration of substrate will drop quickly due to absorption into newly added vesicles. It is reasonable to assume that C_{12} -NBD-PC binds to vesicles with a diffusion-controlled or near-diffusion-controlled rate constant of $\sim 10^8\text{ M}^{-1}\text{ s}^{-1}$ (18). Then, the half-time for uptake of C_{12} -NBD-PC by $2 \times 10^{-8}\text{ M}$ vesicles ($20\text{ }000$ lipids/vesicle) (11) is $\sim 1\text{ s}$. Thus, the results of

Figure 5 (curve b) establish an aqueous mechanism for pPAF-AH. The data with C₁₂-NBD-PC also confirm the energy transfer studies showing that enzyme does not exchange between DMPM vesicles.

These order of addition effects should vanish if substrate undergoes rapid intervesicle exchange regardless of whether the interfacial or aqueous mechanism applies. Indeed, the rate of hydrolysis of C₆-NBD-PC is invariant to the order of addition of components. The following experiments all give the same final turnover number (after addition of all components) within experimental error (not shown): DMPM then enzyme then DMPM/C₆-NBD-PC; DMPM/C₆-NBD-PC then enzyme then DMPM; and DMPM + DMPM/C₆-NBD-PC then enzyme. This series of experiments serves as a control for the C₁₂-NBD-PC results. The same results were obtained with C₁₆- and C₁₈-PAF as substrate, which shows that these natural mediators of inflammation undergo intervesicle exchange on the subminute time scale.

DISCUSSION

A key finding of the present study is that pPAF-AH operates via an aqueous mechanism and interfacial activation, if it occurs, is very modest (<2-fold). The kinetic protocol developed here (Figure 5) for the first time is perhaps the only definitive method for establishing that an enzyme at the interface operates on substrate in the water layer. When neither enzyme nor substrate undergoes intervesicle exchange, as observed for phospholipases A₂ acting on long-chain phospholipids (scooting mode), catalysis under such conditions establishes that vesicle-bound enzyme acts on substrate in the interface (15, 19). Previous workers have shown that bacterial phosphatidylinositol-specific phospholipase C bound to vesicles is capable of hydrolyzing water soluble substrates inositol 1-[4-(nitrophenyl)phosphate] and inositol cyclic phosphate, and the enzyme is activated by the interface (20, 21). Under the assumption that this substrate has virtually zero solubility in the membrane phase, the data suggest that the phospholipase C can operate by the Aq + IFA mechanism, but they do not rule out the possibility that water-soluble substrate must pass through the interface to reach the enzyme's active site. It seems likely that this enzyme operates on its natural substrates, highly water-insoluble long-chain phosphatidylinositols, by the IF or IF + IFA mechanism. Together the results suggest that two fundamentally different mechanisms can be operative for the same enzyme, depending on the membrane solubility of the substrate.

The aqueous mechanism of pPAF-AH readily explains the substrate specificity of this enzyme. The specificity for the acetyl group at the *sn*-2 position of PAF is not absolute. Phosphatidylcholines containing the *sn*-2 propanoyl group and *sn*-2 fatty acyl chains containing several CH₂s with an oxidized carbon at the ω -end are well tolerated by pPAF-AH. This suggests that the acetyl group does not pack into a cul-de-sac-like pocket on the enzyme. It is also difficult to imagine a mechanism based on the structure of the active site that explains the triggering of catalysis by the addition of a polar aldehyde or carboxylic acid at the ω -end of *sn*-2 octanoyl or nonanoyl chains. Finally, it is difficult to imagine a pPAF-AH active site architecture that so dramatically distinguishes between C₁₆- and C₂₄-PAF (Table 2). Clearly

a common feature of all good substrates for pPAF-AH is their relatively high solubility in water compared to naturally occurring phospholipids with two long-chain fatty acids. The demonstration that pPAF-AH must bind substrate in the aqueous phase provides the missing link to understand its substrate specificity. This mode of catalysis also explains the observation that the relative rate of hydrolysis of C₆-NBD-PA, -PS, and -PG is governed not by $^aV_{\max}$ but mainly by the relative substrate partition constants between the aqueous phase and the interface. C₆-NBD-PE is the poorest pPAF-AH substrate, especially in the presence of DMPM, because of a tendency to partition into anionic vesicles, which is consistent with an independent demonstration of favorable phosphatidylethanolamine-DMPM interaction (22), and because of a relatively low $^aV_{\max}$ value. The fact that pPAF-AH tolerates phospholipids with different polar headgroups suggests that it could function to hydrolyze phospholipids of all classes that have undergone oxidative scission of their *sn*-2 fatty acyl chains.

In contrast to pPAF-AH, secreted phospholipases A₂ including the bee venom and porcine pancreatic enzymes are interfacial enzymes that access their substrates from the interface (5). These enzymes contain an active-site slot, and the phospholipid substrate must leave the plane of the membrane and travel about 15 Å to reach the catalytic residues at the end of the slot away from the membrane. These enzymes do not discriminate among substrates with different length *sn*-1 chains (Table 2) or *sn*-2 chains as long the fatty alkyl chains are long enough (>~8 carbons) to extend beyond the length of the slot and remain partially embedded in the bilayer.

Previous workers have suggested that pPAF-AH is an interfacial enzyme (23). This was based on the observation that the action of enzyme on PAF in the absence of vesicles, studied with a fixed time-point assay, showed an anomalous increase in rate when the substrate concentration was increased above its cmc. Using a continuous assay, we see no evidence for such a jump in rate (Figure 3). Regardless of this discrepancy, a jump in rate when substrate concentration exceeds its cmc does not distinguish in any way between interfacial versus aqueous mechanisms. The demonstration that the rate of PAF hydrolysis by pPAF-AH decreases in the presence of detergent (23) is not necessarily due to surface dilution of substrate in the micelle interface. In the context of the Aq and Aq + IFA mechanisms, such a decrease in rate upon addition of detergent would be due to a drop in the solution concentration of substrate as more of it partitions into an increasing number of detergent micelles (mass action, analogous to Figure 4 experiments). Also, inhibition of enzyme by detergent is difficult to rule out.

Given that pPAF-AH operates by an Aq mechanism, the observed saturation behavior in the velocity versus amount of added substrate plots ($^aV_{\max}$, Table 1) does not imply saturation of the active site of enzyme with substrate. To a first approximation, the concentration of PAF or PAF analogue in the aqueous phase in the presence and absence of DMPM and DMPC vesicles cannot exceed its cmc. Thus in the context of the Aq mechanism, the enzymatic rate cannot increase further once the concentration of substrate in the aqueous phase reaches a constant amount determined by its solubility.

Finally, it is difficult to interpret the values of the concentrations of substrates required to achieve 50% of $^aV_{\max}$. Such values are a complex function of the true K_M and of the solubility of substrate in the aqueous phase.

C_{16} -PAF and C_{18} - undergo intervesicle exchange on the subminute time scale (based on experiments analogous to those shown in Figure 5). This dynamic behavior of PAF would explain how it can transfer from cells that produce it to LDL and HDL containing bound pPAF-AH. Presumably, PAF produced on the extracellular face of cells at a site of inflammation remains there long enough to attract PAF receptor-bearing cells that migrate to the injury site only if PAF is continuously biosynthesized. The cell surface PAF concentration will reach a steady-state level determined by its rate of production versus its rate of dissociation into the aqueous phase. Data in Figure 3 (extent of hydrolysis) and Table 1 (substrate concentration required to obtain 50% of $^aV_{\max}$) establish that PAF has no tendency to spontaneously transfer from one side of the bilayer to the other (flip-flop rate half-time > tens of minutes), which argues that PAF produced intracellularly is exposed on the extracellular face of the plasma membrane by a facilitated process.

REFERENCES

1. Barnes, P. J., Page, C. P., and Henson, P. M. (1989) *Platelet Activating Factor and Human Disease*, Blackwell Scientific, Oxford, England.
2. Stafforini, D. M., McIntyre, T. M., Zimmerman, G. A., and Prescott, S. M. (1997) *J. Biol. Chem.* 272, 17895–17898.
3. Tjoelker, L. W., Eberhardt, C., Unger, J., Trong, H. L., Zimmerman, G. A., McIntyre, T. M., Stafforini, D. M., Prescott, S. M., and Gray, P. W. (1995) *J. Biol. Chem.* 270, 25481–7.
4. Scott, D. L., White, S. P., Otwinowski, Z., Yuan, W., Gelb, M. H., and Sigler, P. B. (1990) *Science* 250, 1541–1546.
5. Jain, M. K., Rogers, J., Jahagirdar, D. V., Marecek, J. F., and Ramirez, F. (1986) *Biochim. Biophys. Acta* 860, 435–447.
6. Bayburt, T., and Gelb, M. H. (1997) *Biochemistry* 36, 3216–3231.
7. Eisenberg, S. (1980) *Ann. N.Y. Acad. Sci.* 348, 32–47.
8. Leslie, R. B. (1971) *Biochem. Soc. Symp.* 33, 47–85.
9. Stafforini, D. M., Tjoelker, L. W., McCormick, S. P. A., Vaitkus, D., McIntyre, T. M., Gray, P. W., Young, S. G., and Prescott, S. M. (1999) *J. Biol. Chem.* 274, 7018–7024.
10. Heymans, F., Michel, E., Borrel, M. C., Wichrowski, B., Godfroid, J. J., Convert, O., Coeffier, E., Tence, M., and Benveniste, J. (1981) *Biochim. Biophys. Acta* 666, 230–237.
11. Jain, M. K., and Gelb, M. H. (1991) *Methods Enzymol.* 197, 112–125.
12. Nichols, J. W., and Pagano, R. E. (1982) *Biochemistry* 21, 1720–6.
13. Berg, O. G., Yu, B.-Z., Rogers, J., and Jain, M. K. (1991) *Biochemistry* 30, 7283–7297.
14. Jain, M. K., and Berg, O. (1989) *Biochim. Biophys. Acta* 1002, 127–156.
15. Gelb, M. H., Jain, M. K., Hanel, A. M., and Berg, O. (1995) *Annu. Rev. Biochem.* 64, 653–688.
16. Kramp, W., Pieroni, G., Pinckard, R. N., and Hanahan, D. J. (1984) *Chem. Phys. Lipids* 35, 49–62.
17. Rogers, J., Yu, B. Z., and Jain, M. K. (1992) *Biochemistry* 31, 6056–62.
18. Jain, M. K. (1988) *Introduction to Biological Membranes*, Wiley-Interscience, New York.
19. Jain, M. K., Rogers, J., Jahagirdar, D. V., Marecek, J. F., and Ramirez, F. (1986) *Biochim. Biophys. Acta* 860, 435–47.
20. Volwerk, J. J., Filthuth, E., Griffith, O. H., and Jain, M. K. (1994) *Biochemistry* 33, 3464–3474.
21. Wu, Y., Perisic, O., Williams, R. L., Katan, M., and Roberts, M. F. (1997) *Biochemistry* 36, 11223–11233.
22. Lin, H.-K., and Gelb, M. H. (1993) *J. Am. Chem. Soc.* 115, 3932–3942.
23. Stafforini, D. M., Prescott, S. M., and McIntyre, T. M. (1987) *J. Biol. Chem.* 262, 4223–4230.

BI991149U